Bitlis Eren Üniversitesi Fen Bilimleri Dergisi
BİTLİS EREN UNIVERSITY JOURNAL OF SCIENCE
ISSN: 2147-3129/e-ISSN: 2147-3188
VOLUME: 11 NO: 4 PAGE: 960-970 YEAR: 2022
DOI:10.17798/bitlisfen.1120885

Thermodynamic Analysis of a Combined Gas Turbine ORC Using Some Organic Fluids

Ahmet ELBİR[1*], Feyza AKARSLAN KODALOĞLU[1], Mehmet Erhan ŞAHİN[2]
İbrahim ÜÇGÜL[1]
[1]*Süleyman Demirel Üniversitesi YEKARUM 32260, Isparta/TURKEY*
[2]*Isparta Aplied Science University, Technical Vocational High School, Isparta/TURKEY*
(ORCID: 0000-0001-8934-7665) (ORCID: 0000-0002-7855-8616)
(ORCID: 0000-0003-1613-7493) (ORCID: 0000-0001-9794-0653)

Keywords: ORC, Cascade Expansion Gas Turbine, Energy Analysis, Exergy Analysis.

Abstract
The increase in energy and environmental problems has led us to use sustainable methods for the optimization of energy systems. In this study, an integrated Organic Rankine Cycle (ORC) has been added to the waste heat of a cascade expansion gas turbine in the name of innovative concepts in industrial competition. In this ORC system, mass flow rates, pressure ratios, net powers and thermodynamic calculations of five different fluids (R123, R245fa, R600, R365mfc and R113) were made by operating them with a certain heat load. Accordingly, the ORC net powers of the refrigerants were found to be 15.54kW for R123, 14.78kW for R245fa, 14.71kW for R600, 14.78kW for R365mfc and 15.45kW for R113. With the net power of 51.4kW from the gas turbine, the net power obtained with the R123 refrigerant used in the ORC system is added to 15.54 kW and it has been calculated that it provides a total net power of 66.94kW. The energy efficiency of the designed integrated system was calculated as 66% and the exergy efficiency as 20%. It is seen that the importance of sustainable energy in the optimization of power systems combined with ORC is inevitable.

1. Introduction

The growing and developing world population has brought industrial competition with it. The maximum use of energy in the concept of industrial competition has given rise to innovative concepts. In particular, the sustainable use of waste heat in industry has not only reduced fossil energy consumption but also reduced the risk of global warming. In this context, the use of combined power systems developed by taking advantage of the waste heat of gas turbines has increased considerably. The principle of operation of these systems gets its name from the combination of combined cycle production technologies of both gas and steam power. A combined-cycle power plant is based on the use of both power and hot waste heat from a gas turbine. In some studies in the literature; Lecompte et. al. [1], the integration of an ORC system into a 100 MW Electric Arc Furnace (EAF) was performed. The effects of evaluations based on average heat profiles, a vapor buffer, and optimized state and ORC architectures have been studied. The results have shown that it is very important to take into account the heat. It has been found that an optimized sub-critical ORC system can produce a net electrical output of 752 kW with a steam buffer operating at 25 bar. If combined heating is considered, the ORC system can be optimized to produce 521 kW of electricity, they also found that it provides 4.52 MW of heat. Javanshir et. al. [2], have studied the analysis and optimization of an ORC used as a dip cycle in Brayton/ORC and steam Rankine/ORC combined cycle configurations. Utility scale steam Rankine cycle orc power output may be obtained by adding a dip in and determine the increase in ambient conditions (heat sink temperature) to determine the effect on the growth of a unified power steam Rankine/ORC cycle analysis pinched. The results

*Corresponding author: ahmetelbir@sdu.edu.tr
Receieved: 24.05.2022, Accepted: 01.11.2022

showed that CO_2 and air are the best working fluids for the top coating of the Brayton Cycle. Depending on the exhaust temperature of the topping cycle (Brayton), Iso-butane, R11 and ethanol, which are the preferred working fluids for the ORC cycle, have achieved the highest efficiency in the combined cycle. Ahmadi et. al. [3], investigated the efficiency of solar-powered gas turbines in various parameters such as pressure ratio, turbine inlet temperature, heat sink geometry and component performance. The results showed that a 10% increase in turbine efficiency could lead to a 6-12% improvement in the efficiency of the closed Brayton cycle. Nassar et. al. [4], designed a gas turbine cycle with a thermal efficiency of 34.5% with a target power output of 9 MW. In order to increase the efficiency of the system, an ORC based system was used as a bottom cycle that draws heat from compressed air (intercooler) and exhaust. The pressure ratios, operating pressures and temperatures of the compressors in the ORC system have been optimized using parametric studies. With the addition of decooperation and recovery to this basic system and the inclusion of the dip cycle, they have increased the efficiency to about 47.94%. Kaşka et. al. [5], aimed to investigate the effects of using an ORC as a decoiler on the overall system efficiency in the Brayton cycle. In addition, they investigated the effects of turbine inlet temperature and pressure ratio on system performance. The exergy destruction and exergy efficiency of all components of the combined cycle at different pressure ratios have been calculated. The net power generated by the ORC has been studied depending on the second law efficiency and exergy destruction of the ORC, the second law of the preheater and the exergy destruction. They noted that there is a correlation between the pressure of the Dec Brayton cycle and the net power output. They observed that as the pressure increased, the temperature of the ORC heat source also increased. In addition, they emphasized that increased pressure increases energy and exergy efficiency. Ren et. al. [6], proposed a combined cycle of a gas turbine and an ORC to further improve the energy efficiency of gas turbines. Simulation results have shown that mixtures allow the combined cycle to achieve higher efficiency than pure fluids. They noted that for gas turbines of different power levels, the toluene benzene mixture is more suitable for the recovery of waste heat from small and medium-sized gas turbines, while cyclopentane is more suitable for microgas turbines. Kaşka et. al. [7], carried out a thermodynamic analysis of an ORC using waste heat from the intercooler and regenerator in the Brayton cycle with decooperation, reheating and regeneration (BCIRR) and decooperation. They have revealed various outputs, such as cycle efficiencies in the Brayton cycle depending on turbine inlet temperature, intercooler pressure ratios and decongestant temperature difference. It is emphasized that for all cycles, the net power generated due to the increased turbine inlet temperature has increased. It has been said that since the heat input to the cycles occurs at high temperatures, the net power generated due to the increased turbine input temperature for all cycles increases. They calculated that the thermal efficiency of the combined cycle is about 11.7% higher than the thermal efficiency of the Brayton cycle alone. Blanco et. al. [8], performed thermodynamic, exergy and environmental impact assessments for a Brayton S-CO_2 (supercritical carbon dioxide) cycle combined with ORC. The results showed that the main turbine and the secondary turbine of the Brayton S-CO_2 cycle offer higher exergetic efficiency, 97% and better thermal and energetic behavior compared to other components of the system. Gürgen and Altın [9], have worked on a comprehensive decision-making strategy for the selection of working fluids in ORC applications. The results obtained for 10 different study fluids were evaluated with a comprehensive decision-making strategy. They have designated R245fa as the final working fluid [9]. Chacartegui et al. [10], investigated, low temperature ORC as a dip cycle in medium and large scaled combined cycle power plants by using 8 different refrigerants (R113, R245, isobutene, toluene, cyclohexane, isopentane, toluene and cyclohexane). Competitive results have been achieved for ORC combined cycles with reasonably high global efficiencies. In Khanet et. al. [11], performance analysis of a combined pre-compression supercritical CO_2 cycle and ORC powered by a solar tower for waste heat recovery is studied. It was found that as the heat exchanger efficiency increased, the waste heat recovery rate also increased. The highest heat exchanger efficiency for R227 was found to be 0.95 and the waste heat recovery rate was 0.5673. Carcasci et. al. [12], investigated the optimization of the organic Rankine cycle for four different working fluids (toluene, benzene, cyclopentane and cyclohexane) by changing the main pressure of the fluid at different temperatures of the oil circuit. In Ighodaro et. al. [13], energy analysis of a Combined Regenerative Gas Turbine Organic Rankine Cycle (CRGTORC) was conducted to use the exhaust heat from an existing power plant in Nigeria in their study. The performance of CRGTORC was compared to the current SGT using cyclopentane as the working fluid used in the ORC section. They found that the CRGTORC model increased the net power output, thermal efficiency, total cycle efficiency and operating rate of the system

by 23.53%, 62.24%, 54.60% and 10.21%, respectively. Flue gas losses, specific fuel consumption and heat rate decreased by 89.21%, 36.26% and 36.26%, respectively. In addition, it has been observed that the increase in compressor inlet air temperature causes an increase in the specific fuel consumption and heat rate and causes a decrease in net power output, thermal efficiency, cycle efficiency, flue gas losses and work rate. Mishra and Kuamar [14], developed a performance equation for three working fluids (R123, R245fa and R134a) to improve the thermodynamic performance of the brayton cycle. They observed that the Brayton cycle working with R123 gave better thermodynamic performances. Jeong et. al. [15], developed a new cycle with three different refrigerants (R123, R134a and R245ca) Rankine and refrigeration cycles and a thermodynamic analysis of the system was made. It was found that the cycle using R123 refrigerant gave the highest cycle efficiency among all cycles. In Lei et. al. [16], performance evaluation of SRC and ORC systems, which are used as bottom systems in a, GT-based combined system, has been conducted for different turbine inlet temperatures and pressures. As a result, R141b was found as the best working refrigerant. They found the maximum net thermal efficiency, exergy efficiency and net power of ORC with R141b as 22.6%, 64.76% and 780.35 kW at 40 bar and 225 °C, respectively. They found the net thermal and exergy efficiency of the overall system (GT-SRC-ORC) with R141b to be 47.65% and 67.35%, respectively. In this case, they determined that waste heat recovery was realized, corresponding to 734.57 kg/h natural gas, which is equivalent to 2203.73 kg-CO_2/h emissions.

In this study, it is aimed to produce electricity again in the ORC cycle by comparing ORC cycle with fluids with different high critical temperatures (R113, R123, R245fa, R365mcf and R600) in the heat remaining after transferring eventual heat energy received from a heat source to a gas turbine-designed system and generating electricity with turbines..

2. Material and Method

2.1. Cascade Expansion Gas Turbine

The cascade expansion gas turbine cycle is shown in figure 1. Accordingly, in state 1, air at atmospheric pressure enters the compressor. The air should be state 2 with increased pressure and temperature being transferred to it should be state 3 with the high heat it receives from the heat source. In case 4, a 1/3 cascade expansion was made in the turbine. In the case of 5, the cascade expanding air is reduced to atmospheric pressure and its output is provided.

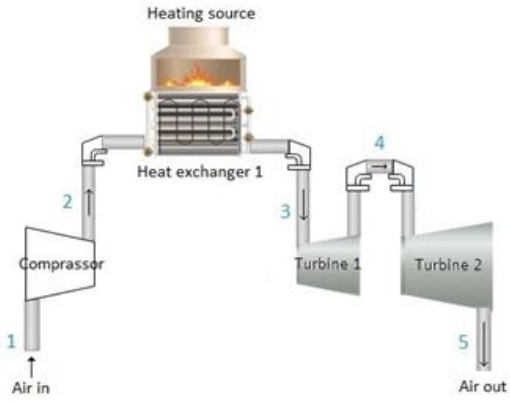

Figure 1. Cascade expansion gas turbine system.

2.2. Model Description

The designed system is shown in Figure 2. The ORC system is integrated into the gas turbine waste heat with step expansion. The step-expansion gas turbine has been described above (Fig. 1). The waste heat received by the ORC system heat exchanger is at 10, and the hot refrigerant expands and generates electricity from the turbine. In 11 cases, heat transfer occurs by condensation thanks to the heat exchanger. In state 7, the fluid, which is saturated liquid, enters the pump and its pressure is increased, and the cycle is completed.

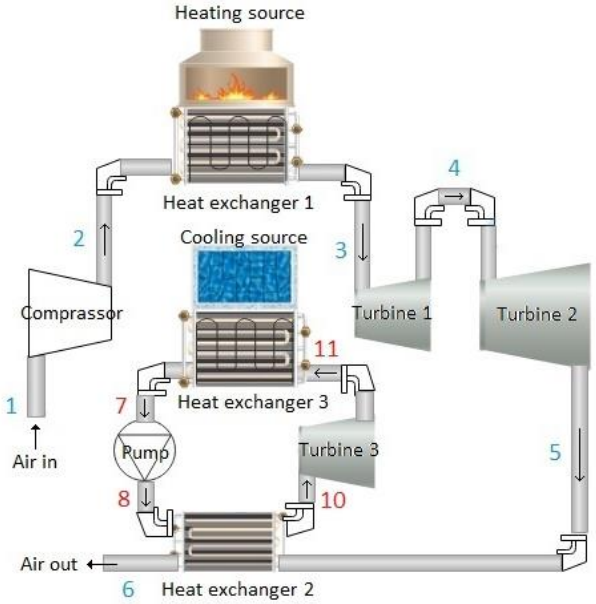

Figure 2. Design of the unified power system.

Assumptions and fixed parameters;

- All components in the system neglect the pressure losses that may occur in the pressure line.

- Their changes in kinetic and potential energy was neglected.
- The heat exchange coefficient was accepted as 1.4. (source of heat = heat entering the system*1,4)
- The instantaneous temperature difference coefficient between the heat sources and the heat exchanger surfaces was accepted as 1.1. (heat source surfaces temperature = heat surfaces temperature entering the system *1.1)
- The source temperatures used in the ORC system were kept constant as 385.5 K for the evaporator (HX2) and 318.8 K for the condenser (HX3).
- The isentropic efficiency of the turbines in the entire system was calculated as 90%, and the isentropic efficiency of the pump and compressor was calculated as 80%.
- The pressure ratio of the turbines that make gradual expansion in the gas turbine cycle was taken as 1/3.
- In the step-expansion gas turbine and ORC system, the flows were assumed to be constant mass flow.
- The dead state was taken at 20 ^{0}C.
- System components are Adiabatic.

2.3. Thermodynamic Analysis

The equations used according to the laws of thermodynamics are as follows:

For the steady state in thermodynamic analysis, the basic equation of mass balance is as follows;

$$\sum \dot{m}_{in} = \sum \dot{m}_{ex} \quad (1)$$

where $\dot{m}$ denotes the mass flow rate, and the in and ex indices denote the input and output states, respectively. The energy balance is:

$$\dot{Q}_{in} + \dot{W}_{in} + \sum_{in} \dot{m}\left(h + \frac{V^2}{2} + gz\right) = \dot{Q}_{ex} + \dot{W}_{ex} + \sum_{ex} \dot{m}\left(h + \frac{V^2}{2} + gz\right) \quad (2)$$

Where $\dot{Q}$ is the heat transfer rate, $\dot{W}$ is the power, h is the specific enthalpy, v is the speed, z is the height, and g is the gravitational acceleration. The entropy equilibrium equation for steady-state conditions is written as:

$$\sum_{in} \dot{m}_{in} s_{in} + \sum_k \frac{\dot{Q}}{T_k} + \dot{S}_{gen} = \sum_{ex} \dot{m}_{ex} s_{ex} \quad (3)$$

where s is the specific entropy and $\dot{S}_{gen}$ is the production rate of entropy. The equation of exergy balance:

$$\sum \dot{m}_{in}\, ex_{in} + \sum \dot{E}\, x_{Q,in} + \sum \dot{E} x_{W,in} = \sum \dot{m}_{ex} ex_{ex} + \sum \dot{E} x_{Q,ex} + \sum \dot{E} x_{W,ex} + \dot{E} x_D \quad (4)$$

Specific flow exergy:

$$ex = x_{ph} + ex_{ch} + ex_{pt} + ex_{kn} \quad (5)$$

The kinetic and potential parts of the exergy have been processed with the assumption that they are negligible. It is also assumed that the chemical exergy is negligible. The physical or flow exergy (ex_{ph}) is defined as:

$$ex_{ph} = (h - h_o) - T_o(s - s_o) \quad (6)$$

where h and s represent the specific enthalpy and entropy, respectively, in the real case. h_o and s_o symbolize the enthalpy and entropy in the reference ambient states, respectively.

The destruction (D) of exergy is equal to the product of mass with specific exergy;

$$\dot{E} x_D = ex * m \quad (7)$$

$\dot{E} x_D$ are the work-related exergy ratios and are given by:

$$\dot{E} x_D = T_0 \dot{S}_{gen} \quad (8)$$

$\dot{E} x_W$ are the work-related exergy ratios and are given by:

$$\dot{E} x_W = \dot{W} \quad (9)$$

$\dot{E} x_Q$, exergy destruction rate related to heat transfer is given as below.

$$\dot{E} x_Q = \left(1 - \frac{T_o}{T}\right) \dot{Q} \quad (10)$$

What is the work that comes out of the system.

$$\dot{W} net_{out} = \dot{Q}_{in} - \dot{Q}_{out} \quad (11)$$

The energy efficiency (η) for the system;

$$\eta th = \frac{\dot{W}net_{out}}{\dot{Q}_{in}} \quad (12)$$

The exergy efficiency (ψ) can be defined as follows;

$$\psi = \frac{\sum useful\ output\ exergy}{\sum input\ exergy} = 1 - \frac{\sum exergy\ loss}{\sum input\ exergy} \quad (13)$$

The instantaneous temperature T(K) value for surfaces was calculated as:

$$T = \frac{h_2 - h_1}{s_2 - s_1} \quad (14)$$

In Table 1, the mass balance, energy balance, entropy balance, exergy balance and exergy yields for each component are presented separately [18], [19]

Table 1. The Gas Turbine and ORC Combined Cycle equilibrium equations

Component	Mass balance	Energy balance	Entropy balance	Exergy balance	Exergy efficiency
Air-Comp. (1-2)	$\dot{m}_1 = \dot{m}_2 = \dot{m}_{air}$	$\dot{W}_{Comp1.} = \dot{m}_{air}(h_2 - h_1)$	$\dot{S}_{gen,Comp1.} = \dot{m}_{air}(s_2 - s_1)$	$\dot{E}x_{D,Comp1} = \dot{m}_{air}(ex_1 - ex_2) + \dot{W}_{Comp1}$	$\psi_{copm1} = \frac{\dot{m}_{air}(ex_2 - ex_1)}{\dot{W}_{Comp1}}$
Air-heat exchanger I (2-3)	$\dot{m}_2 = \dot{m}_3 = \dot{m}_{air}$	$\dot{Q}_{HXI}^{in} = \dot{m}_{air}(h_2 - h_3)$ $\dot{Q}_{HX1}^{out} = \dot{m}_{air}(h_2 - h_3)/1{,}4$	$\dot{S}_{gen.,HX1} = \dot{m}_{air}(s_2 - s_3) + \left(\frac{\dot{Q}_{air}^{out}}{T_{HX1} * 1{,}1}\right)$	$\dot{E}x_{D,HX1} = \dot{m}_{air}(ex_2 - ex_3) - \dot{Q}_{air}^{out}\left(1 - \frac{T_0}{T_{HX1} * 1{,}1}\right)$	$\psi_{HX1} = \frac{\dot{Q}_{air}^{out}\left(1 - \frac{T_0}{T_{HX1} * 1{,}1}\right)}{\dot{m}_{air}(ex_2 - ex_3)}$
Air-Turbine I (3-4)	$\dot{m}_3 = \dot{m}_4 = \dot{m}_{air}$	$\dot{W}_{turb1.} = \dot{m}_{air}(h_3 - h_4)$	$\dot{S}_{gen,turb1.} = \dot{m}_{air}(s_4 - s_3)$	$\dot{E}x_{D,turb1.} = \dot{m}_{air}(ex_3 - ex_4) - \dot{W}_{turb1.}$	$\psi_{turb1.} = \frac{\dot{W}_{turb1.}}{\dot{m}_{air}(ex_3 - ex_4)}$
Air-Turbine II (4-5)	$\dot{m}_4 = \dot{m}_5 = \dot{m}_{air}$	$\dot{W}_{turb2.} = \dot{m}_{air}(h_4 - h_5)$	$\dot{S}_{gen,turb2.} = \dot{m}_{air}(s_5 - s_4)$	$\dot{E}x_{D,turb2.} = \dot{m}_{air}(ex_4 - ex_5) - \dot{W}_{turb2.}$	$\psi_{turb2.} = \frac{\dot{W}_{turb2.}}{\dot{m}_{air}(ex_4 - ex_5)}$
Air-ORC heat exchanger II (5-6) (8-10)	$\dot{m}_5 = \dot{m}_6 = \dot{m}_{air}$; $\dot{m}_8 = \dot{m}_{10} = \dot{m}_{orc}$	$\dot{Q}_{orc}^{in} = \dot{m}_{orc}(h_6 - h_5)/1{,}4$	$\dot{S}_{gen.,HX2} = \dot{m}_{air}(s_6 - s_5) - \dot{m}_{orc}(s_{10} - s_8)$	$\dot{E}x_{D,HX2} = \dot{m}_{air}(ex_5 - ex_6) - \dot{m}_{orc}(ex_8 - ex_{10})$	$\psi_{HX2} = \frac{\dot{m}_{orc}(ex_5 - ex_6)}{\dot{m}_{air}(ex_8 - ex_{10})}$
ORC-Turbine III (10-11)	$\dot{m}_{10} = \dot{m}_{11} = \dot{m}_{orc}$	$\dot{W}_{turb3.} = \dot{m}_{orc}(h_{10} - h_{11})$	$\dot{S}_{gen,turb3.} = \dot{m}_{orc}(s_{11} - s_{10})$	$\dot{E}x_{D,turb3.} = \dot{m}_{orc}(ex_{10} - ex_{11}) - \dot{W}_{turb3.}$	$\psi_{turb3.} = \frac{\dot{W}_{turb.}}{\dot{m}_{orc}(ex_{10} - ex_{11})}$
ORC heat exchanger III (7-11)	$\dot{m}_{11} = \dot{m}_7 = \dot{m}_{orc}$	$\dot{Q}_{HX3}^{in} = \dot{m}_{orc}(h_{11} - h_7)$ $\dot{Q}_{orc}^{out} = \dot{m}_{orc}(h_{11} - h_7)/1{,}4$	$\dot{S}_{gen.,HX3} = \dot{m}_{orc}(s_7 - s_{11}) + \left(\frac{\dot{Q}_{orc}^{out}}{T_{HX3}/1{,}1}\right)$	$\dot{E}x_{D,HX3} = \dot{m}_{orc}(ex_{11} - ex_7) - \dot{Q}_{orc}^{out}\left(1 - \frac{T_0}{T_{HX3}/1{,}1}\right)$	$\psi_{HX3} = \frac{\dot{Q}_{orc}^{out}\left(1 - \frac{T_0}{T_{HX3}/1{,}1}\right)}{\dot{m}_{orc}(ex_{11} - ex_7)}$
ORC-pump (7-8)	$\dot{m}_7 = \dot{m}_8 = \dot{m}_{orc}$	$\dot{W}_{pump} = \dot{m}_{orc}(h_8 - h_7)$	$\dot{S}_{gen,pump} = \dot{m}_{orc}(s_8 - s_7)$	$\dot{E}x_{D,pump} = \dot{m}_{orc}(ex_7 - ex_8) + \dot{W}_{pump}$	$\psi_{pump} = \frac{\dot{m}_{orc}(ex_7 - ex_8)}{\dot{W}_{pump}}$

3. Results and Discussion

Figure 3 shows the T-s (temperature enthalpy) diagram for the Brayton cycle.

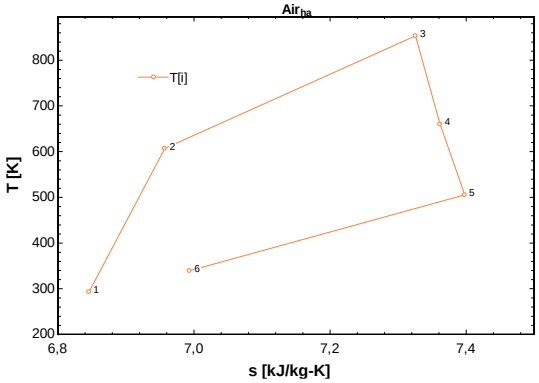

Figure 3. Air cascade expansion gas turbine cycle T-s diagram

In Figure 3, the temperature that changes with the flow direction of the fresh air entering from the 1st point is presented in the temperature-entropy diagram.

The thermodynamic values in Figure 1 for the cascade expansion gas turbine cycle are presented in Table 2. The T_0 point indicates the dead state.

Table 2. Point values in the cascade expansion gas turbine cycle

Cascade-Air	T [K]	s kJ/kg.K	P [bar]	h [kJ/kg]	Ex [kJ/kg]	m [kg/s]
1	293.2	6.846	1	293.4	0	1
2	607.1	6.957	9	614.7	288.6	1
3	853.2	7.325	9	881.4	447.4	1
4	659.3	7.362	3	670.7	226	1
5	505.3	7.398	1	508.8	53.5	1
6	339.6	6.994	1	340.1	3.347	1
T_0	293.2	6.846	1	293.4		

Thermodynamic calculations for the cascade expansion gas turbine cycle are given in Table 3.

Table 3. Thermodynamic consequences of the cascade expansion gas turbine cycle

Cascade-Air	Ex(KW)	Q(KW)in	Q(KW)out	W(KW)	φ
1-2 Compressor	32.72	-	-	321.3	0.90
2-3 Heat exchanger 1	77.23	266.7	373.4	-	0.67
3-4 Turbine1	10.58	-	-	210.8	0.95
4-5 Turbine2	10.62	-	-	161.9	0.94
5-6 Heat exchanger 2	25.07	120.5	168.7	-	0.5

As can be seen in Table 3, the exergy loss for the cascade expansion gas turbine cycle was highest in heat exchanger 1, followed by compressor, heat exchanger 2, turbine 2 and turbine 1. In addition, the heat exchangers are exchanged with a difference of 1.4 heat exchange coefficient from the source, the compressor and turbine power loads and the exergy efficiencies of each component are presented. The total net power was found to be 51.4 kW by subtracting the energy consumed for the compressor from the sum of the powers obtained from Turbine 1 and Turbine 2 (Table 3).

Figure 4-8 shows the T-s diagram for the heat cycle obtained from waste heat combined with an ORC system for refrigerants R600, R113, R 245fa, R 365mfc and R 123.

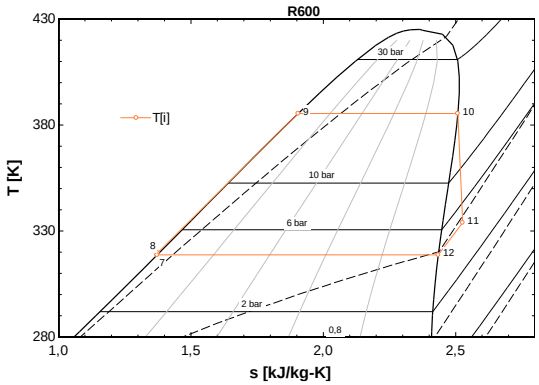

Figure 4. T-s diagram for ORC R600

Thermodynamic values of the ORC for the R 600 are presented in Table 4.

Table 4. Thermodynamic values for ORC-R600

ORC-R600	T [K]	s kJ/kg.K	P [bar]	h [kJ/kg]	Ex [kJ/kg]	m [kg/s]
7	318.7	1.372	4.415	310.7	9.284	0.2869
8	319.8	1.374	19.27	314.1	10.08	0.2869
9	385.5	1.905	19.27	501.5	19.19	0.2869
10	385.5	2.508	19.27	734	35.15	0.2869
11	333.9	2.527	4.415	679.4	17.94	0.2869
12	318.7	2.435	4.415	649.3	17.06	0.2869
T_0		2.532		618.5		

Thermodynamic calculations for the ORC system are given in Table 5.

Table 5. Thermodynamic results for ORC system R600 refrigerant

ORC-R600	Ex(KW)	Q(KW)in	Q(KW)out	W(KW)	φ
7-8 Pump	0.178	-	-	0.970	0.81
8-10 Heat exchanger 2	25.07	120.5	168.7	-	0.50
10-11 Turbine3	1.54	-	-	15.68	0.91
11-12 Heat exchanger 3	21.14	105.7	75.55	-	0.69

As can be seen in Table 5, the exergy loss for the ORC system is highest in heat exchanger 3, followed by heat exchanger 4, turbine 3 and pump. In addition, the heat exchangers are exchanged with a difference of 1.4 heat exchange coefficient from the

source; the compressor and turbine power loads and the exergy efficiencies of each component are presented.

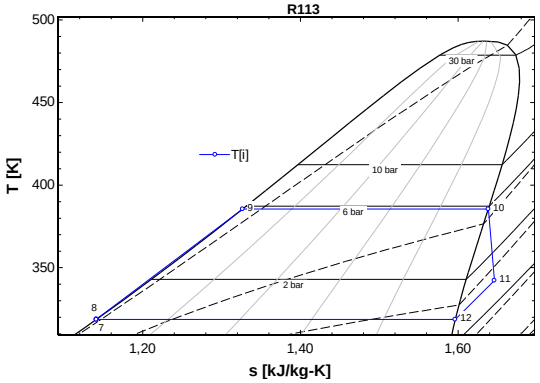

Figure 5. T-s diagram for ORC R113

Thermodynamic values for the ORC cycle are presented in Table 6.

Table 6. Thermodynamic values for ORC-R113

ORC-R113	T [K]	s kJ/kg.K	P [bar]	h [kJ/kg]	Ex [kJ/kg]	m [kg/s]
7	318.7	1.141	0.9463	241.8	0.539	0.6505
8	318.9	1.142	5.781	242.2	0.751	0.6505
9	385.5	1.327	5.781	307.3	7.786	0.6505
10	385.5	1.638	5.781	427.4	26.5	0.6505
11	342.3	1.646	0.9463	403.3	9.289	0.6505
12	318.7	1.596	0.9463	386.8	8.086	0.6505
T_0		1.064		218.3		

Thermodynamic calculations for the ORC system are given in Table 7.

Table 7. Thermodynamic results for ORC system R113 refrigerant

ORC-R113	Ex(KW)	Q(KW)in	Q(KW)out	W(KW)	φ
7-8 Pump	0.047	-	-	0.26	0.81
8-10 Heat exchanger 2	24.4	120.5	168.7	-	0.51
10-11 Turbine3	1.54	-	-	15.71	0.91
11-12 Heat exchanger 3	21.25	105.7	75.55	-	0.70

As seen in Table 7, the exergy loss for the ORC system is highest in heat exchanger 3, followed by heat exchanger 4, turbine 3 and pump. In addition, the heat exchangers are exchanged with a difference of 1.4 heat exchange coefficient from the source, the compressor and turbine power loads and the exergy efficiencies of each component are presented.

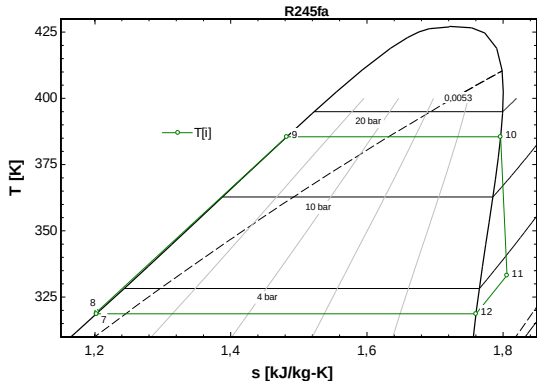

Figure 6. T-s diagram for ORC R245fa

Thermodynamic values for the ORC cycle are presented in Table 8.

Table 8. Thermodynamic values for ORC-R245fa

ORC-R245fa	T [K]	s kJ/kg.K	P [bar]	h [kJ/kg]	Ex [kJ/kg]	m [kg/s]
7	318.7	1.203	2.987	260.2	2.809	0.5493
8	319.5	1.204	16.53	261.5	3.4	0.5493
9	385.5	1.482	16.53	359.7	12.49	0.5493
10	385.5	1.796	16.53	480.8	28.43	0.5493
11	333.2	1.806	2.987	452.6	11.4	0.5493
12	318.7	1.203	2.987	260.2	2.809	0.5493
T_0		1.766		420.1		

Thermodynamic calculations for the ORC system are given in Table 9.

Table 9. Thermodynamic results for ORC system R245fa refrigerant

ORC-R245fa	Ex(KW)	Q(KW)in	Q(KW)out	W(KW)	φ
7-8 Pump	0.13	-	-	0.72	0.81
8-10 Heat exchanger 2	25.13	120.5	168.7	-	0.50
10-11 Turbine3	1.52	-	-	15.5	0.91
11-12 Heat exchanger 3	21.04	105.7	75.55	-	0.69

As seen in Table 9, the exergy loss for the ORC system is highest in heat exchanger 3, followed by heat exchanger 4, turbine 3 and pump. In addition, the heat exchangers are exchanged with a difference of 1.4 heat exchange coefficient from the source, the compressor and turbine power loads and the exergy efficiencies of each component are presented.

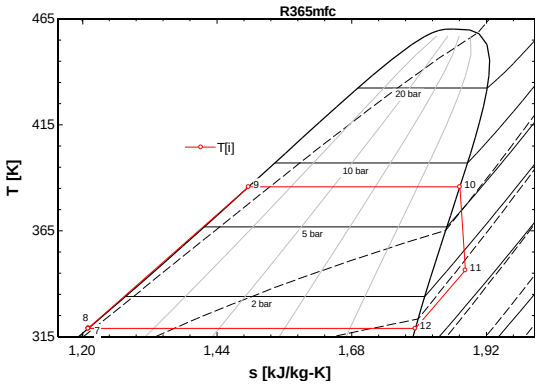

Figure 7. T-s diagram for ORC R365mfc

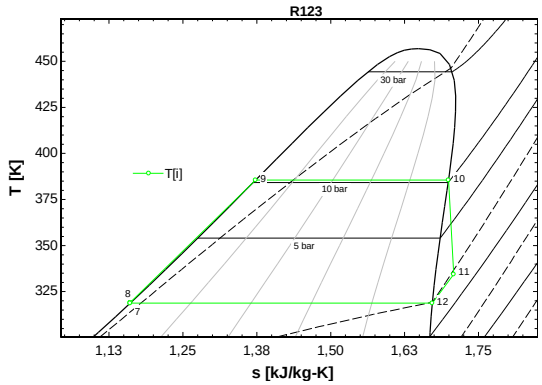

Figure 8. T-s diagram for ORC R123

Thermodynamic values for the ORC cycle are presented in table 10.

Table 10. Thermodynamic values for ORC- R365mfc

ORC-R365mfc	T [K]	s kJ/kg.K	P [bar]	h [kJ/kg]	Ex [kJ/kg]	m [kg/s]
7	318.7	1.211	1.224	262.4	0.674	0.4909
8	318.9	1.211	7.825	263	0.946	0.4909
9	385.5	1.496	7.825	363.4	9.17	0.4909
10	385.5	1.873	7.825	508.5	26.22	0.4909
11	346.2	1.883	1.224	477.7	9.681	0.4909
12	318.7	1.793	1.224	262.4	0.674	0.4909
T_0		1.095		227		

Thermodynamic calculations for the ORC system are given in Table 11.

Table 11. Thermodynamic results for ORC system R365mfc refrigerant

ORC-R365mfc	Ex(KW)	Q(KW)in	Q(KW)out	W(KW)	φ
7-8 Pump	0.06	-	-	0.33	0.81
8-10 Heat exchanger 2	24.88	120.5	168.7	-	0.50
10-11 Turbine3	1.43	-	-	15.11	0.91
11-12 Heat exchanger 3	21.72	105.7	75.55	-	0.70

As can be seen in Table 11, the exergy loss for the ORC system is highest in heat exchanger 3, followed by heat exchanger 4, turbine 3 and pump. In addition, the heat exchangers are exchanged with a difference of 1.4 heat exchange coefficient from the source, the compressor and turbine power loads and the exergy efficiencies of each component are presented.

Thermodynamic values for the ORC cycle are presented in table 12.

Table 12. Thermodynamic results for ORC system R123 refrigerant

ORC-R123	T [K]	s kJ/kg.K	P [bar]	h [kJ/kg]	Ex [kJ/kg]	m [kg/s]
7	318.7	1.161	1.851	247.8	0.752	0.6008
8	319.2	1.161	10.27	248.5	1.119	0.6008
9	385.5	1.373	10.27	323.4	8.82	0.6008
10	385.5	1.699	10.27	449.1	26.89	0.6008
11	334.4	1.708	1.851	422.4	9.336	0.6008
12	318.7	1.672	1.851	410.5	8.573	0.6008
T_0		1.074		221.1		

Thermodynamic calculations for the ORC system are given in Table 13.

Table 13. Thermodynamic results for ORC system R245fa refrigerant

ORC-R123	Ex(KW)	Q(KW)in	Q(KW)out	W(KW)	φ
7-8 Pump	0.08	-	-	0.45	0.81
8-10 Heat exchanger 2	24.38	120.5	168,7	-	0.51
10-11 Turbine3	1.56	-	-	15.99	0.91
11-12 Heat exchanger 3	20.98	105.7	75.55	-	0.69

As can be seen in Table 13, the exergy loss for the ORC system is highest in heat exchanger 3, followed by heat exchanger 4, turbine 3 and pump. In addition, the heat exchangers are exchanged with a difference of 1.4 heat exchange coefficient from the source, the compressor and turbine power loads and the exergy efficiencies of each component are presented.

The energy and exergy efficiencies of ORC and gas turbine cycles are given in Table 14. In addition, the net power, high and low pressure ratios in the ORC system and the amount of fluid used in the system are also presented.

Table 14. Energy and exergy efficiencies, ORC mass and net power in GT and ORC system

Fluid	$\frac{P_{10}}{P_{11}}$	$\dot{W}_{NET,ORC} = \dot{W}_{Turb,ORC} - \dot{W}_{Pump,ORC}$	ORC mass ($\dot{m}$)	Energy efficiencies (GT+ORC)	Exergy efficiencies (GT+ORC)
R 600	4.36	14.71	0.2869	0,66	0,20
R113	6.11	15.45	0.6505	0,66	0,20
R245fa	5.53	14.78	0,5493	0,66	0,20
R365mfc	6.39	14.78	0,4909	0,66	0,20
R123	5.55	15.54	0,6008	0,66	0,20

120.5 kW of the 168.7 kW (120.5*1.4) of heat output from the step-expansion gas turbine was used as useful heat for the ORC system. This was compared by applying it to five different fluids as shown in Table 15. In terms of mass flow rates of the refrigerants used in ORC, at least R600 refrigerant was used and at most R113 refrigerant was used. When looking at the condenser and evaporator pressure ratios in ORC, it was found that at least R600 and at most R365mfc refrigerants. 51.4 kW net power from the cascade gas turbine and 15.54 kW net power from the downcycle R123 refrigerant system of the cascade gas turbine (as shown in table 14). Total energy efficiencies of 66% and exergy 20% of GT and ORC cycles remained constant.

4. Conclusion and Suggestions

In this study, the thermodynamic analysis of the gas turbine (GT) system integrated into a heat source and the Organic Rankine Cycle (ORC) systems integrated into the turbine waste heat of this gas turbine system were made. Thermodynamic calculations were made using the waste heat of 120.5 kW corresponding to the ORC system, five different refrigerants with high critical temperature (R123, R245fa, R600, R365mfc and R113) as the working fluid in the cycle. The heat exchangers are exchanged with a difference of 1.4 heat exchange coefficient from the source, the compressor and turbine power loads and the exergy efficiencies of each component are presented. Engineering Equation Solver (EES) program was used for thermodynamic analysis [20]. According to the results obtained;

- The gas turbine cycle worked with 16% efficiency. The most exergy loss was in heat exchanger 1, which is the main heat source, followed by the air inlet compressor, ORC heat transfer heat exchanger 2, turbine 2 and turbine 1.
- When evaluated in terms of mass flow rates of the refrigerants used in ORC, at least R600 refrigerant was used and at most R113 refrigerant was used.
- When looking at the condenser and evaporator pressure ratios in ORC, it was found that the refrigerants were at least R600 and at most R365mfc.
- Calculated as R123 refrigerant in terms of net power obtained in the ORC system.
- Total energy efficiencies of 66% and exergy 20% of GT and ORC cycles remained constant.

The result of competitive technologies brings competitive approaches. In this context, providing more power generation from waste heat sources will provide added value to both our national economy and our national energy policies. Alternative integrated system designs and applications will offer more possibilities in this contex

Conflict of Interest Statement

There is no conflict of interest between the authors.

Statement of Research and Publication Ethics

The study is complied with research and publication ethics

References

[1] S. Lecompte, O. A. Oyewunmi, C. N. Markides, M. Lazova, A. Kaya, Van den Broek, M., and De Paepe, M., “Case study of an organic rankine cycle (ORC) for waste heat recovery from an electric arc furnace (EAF)”, *Energies*, 10(5), pp. 649, 2017.

[2] A. Javanshir, N. Sarunac and Z. Razzaghpanah, “Thermodynamic analysis of ORC and its application for waste heat recovery”, *Sustainability*, 2017, (11), 1974.

[3] M. H. Ahmadi, M. N. Alhuyi, R. Ghasempour, F. Pourfayaz, M. Rahimzadeh and T. Ming, "A review on solar assisted gas turbines", *Energy Science & Engineering*, vol. 6, pp. 658-674, 2018.
[4] A. Nassar, N. Mehta, O. Rudenko, L. Moroz, and G. Giri, "Design of Waste Heat Recovery System based on ORC for a Locomotive Gas Turbine",2018.
[5] Ö. Kaşka, B. O. R Onur, N. Tokgöz and M.M. Aksoy, "First and second law evaluation of combined Brayton-Organic Rankine power cycle", *Journal of Thermal Engineering*, vol.4, pp.577-591, 2020.
[6] J. Ren, Y. Cao, Y. Long, X. Qiang and Y. Dai, "Thermodynamic comparison of gas turbine and ORC combined cycle with pure and mixture working fluids", *Journal of Energy Engineering*, 145(1), 05018002, 2019.
[7] Ö. Kaşka, B. O. R. Onur, Tokgöz, N., and Aksoy, M. M., "First and second law evaluation of combined Brayton-Organic Rankine power cycle", *Journal of Thermal Engineering*, vol.6(4), pp.577-591, 2020.
[8] E. B. Espinel, G. O. Valencia and J. F. Duarte, "Thermodynamic, exergy and environmental impact assessment of S-CO_2 brayton cycle coupled with ORC as bottoming cycle". *Energies*, vol.13(9), pp. 2259, 2020.
[9] S. Gürgen and İ. Altin, "Novel decision-making strategy for working fluid selection in Organic Rankine Cycle: A case study for waste heat recovery of a marine diesel engine", *Energy*, 124023, 2022.
[10] R. Chacartegui, D. Sánchez, J. M. Muñoz and T. Sánchez, "Alternative ORC bottoming cycles for combined cycle power plants", *Applied Energy*, vol.86(10), pp.2162-2170, 2009.
[11] Y. Khan and R. S. Mishra, "Performance evaluation of solar based combined pre-compression supercritical CO_2 cycle and organic Rankine cycle", *International journal of Green energy*, vol. 18(2), pp. 172-186, 2021.
[12] C. Carcasci, R. Ferraro and E. Miliotti, "Thermodynamic analysis of an organic Rankine cycle for waste heat recovery from gas turbines", *Energy*, vol.65, pp.91-100, 2014.
[13] O. Ighodaro, P. Ochornma and H. Egware, "Energy Analysis of A Retrofitted Regenerative Gas Turbine Organic Cycle in Ihovbor Power Plant", *International Journal of Engineering Technologies IJET*, vol.6(3), pp.45-61, 2020.
[14] R. M. Mishra and M. Kumar, "Thermodynamic analysis of brayton cycle for power generation", 2019
[15] J. Jeong and Y. T. Kang, "Analysis of a refrigeration cycle driven by refrigerant steam turbine", *International journal of refrigeration*, vol.27(1), pp.33-41,2004.
[16] Y. Lei, S. Ye, Y. Xu, C. Kong, C. Xu, Y. Chen and H. Xiao, "Multi-objective optimization and algorithm improvement on thermal coupling of SOFC-GT-ORC integrated system", *Computers & Chemical Engineering*, 164, 107903, 2022.
[18] I. Dincer and M. A. Rosen, "Exergy: energy, environment and sustainable development", Newnes, 2012.
[19] Y. A. Cengel, M. A. Boles and M. Kanoğlu, "Thermodynamics: an engineering approach", *New York: McGraw-hill*, vol. 5, pp. 445, 2011.
[20] S. A. Klein and F. L. Alvarado, Engineering equation solver. F-Chart Software, Madison, WI, 1,2022.